Mapping wear mechanisms for TiC/Ti composite coatings

G. Rasool, S. Mridha and M.M. Stack*[1]

Department of Mechanical and Aerospace Engineering

University of Strathclyde,

James Weir Building, 75 Montrose St.,

Glasgow, G1 1XJ

***Corresponding author, margaret.stack@strath.ac.uk; Tel: 441415483754; Fax 44141 5525105**

Abstract

In this work, a fundamental study of the wear transition regimes with respect to sliding speed and normal load was carried out for a pin-on-disk sliding couple, involving hardened steel (disks) and titanium base titanium carbide composite coatings (pins). The coating was deposited using a Tungsten Inert Gas (TIG) welding torch melting process. The sliding speed was varied from 0.38 to 1.5m s-1, and the normal load was varied from 10 to 50N. Dry sliding wear behaviour of the disks was characterized by abrasive-oxidative wear at lower normal loads while adhesive-oxidative wear predominated at higher loads with iron oxide transfer to the TiC composite coated pins. In contrast, micro-polishing and adhesive wear predominated for the TiC composite coatings pins along with very mild abrasive wear in evidence. However, the wear regime depended on the conditions with a range of transitions observed over the sliding speeds and loads tested. Wear maps have been constructed to represent the wear mode transitions and the observed wear mechanisms have been discussed.

Keywords: pin-on-disk, TiC coatings, sliding speed, normal load, wastage maps

1. Introduction

The applications of titanium and its alloys are continuously increasing in the aerospace and chemical industries together with the power engineering, and biomedical areas due to their favourable properties such as high strength, low density, good high temperature properties, biocompatibility and favourable corrosion resistance [1-2]. Titanium and its alloys, however, suffer from tribological limitations such as high coefficient of friction, relatively low hardness and sometimes unfavourable wear resistance which have limited their wider application [2]. Through surface engineering, the potential applications of the surface treated titanium can be increased by improving tribological properties [1]. These techniques include thermal spray [3], electron beam [4], laser processing [5], physical vapour deposition

[1] This is the peer-reviewed and accepted author manuscript, to be published in Wear (ISSN: 0043-1648) during 2015.

(PVD), chemical vapour deposition (CVD) [6] and ion implantation. Laser and electron beam processing methods can produce thick coatings which are suitable for tribological applications. These coatings methods and techniques may involve high vacuum. To overcome such problems, various researchers have used the TIG process to produce hard coatings on different substrates [7-8]. This metal coating technique has significant advantages compared to the methods mentioned above in the ease of operation and application. This technique has been used to produce Ti based TiC composite coatings samples in this study.

Titanium carbide coatings have a broad range of industrial as well as biomedical applications because of their very high melting point and thermal stability, low coefficient of friction, high electrical and thermal conductivities, low density, high hardness and high wear and corrosion resistance and good bio-compatibility. TiC composite coatings offer significantly increased wear resistance and chemical stability deposited on titanium substrates as they provide for homogeneous granular surface (structural continuity) compared to other substrates [9-10].

A systematic approach to examine the observations of a wear system over wide range of sliding speed and normal load was first adopted by Welsh in the studies on mild steel sliding wear [11]. He observed the order of magnitude changes in the wear rate and wear mechanism with small changes in normal load or sliding speed Further, wear mechanism map approaches have been adopted for a wide variety of material combinations including steel-on-steel [12], steel against nitride steel [13], ceramic wear [14], aluminium alloys [15], aluminium metal matrix composites [16], TiN-coated high speed steel [17-18] and in previous work by current authors for a 303 substrate coated with TiC [19]. The effect of frictional heating on the sliding wear mechanisms such as oxidation and seizure has also received much attention in the literature [12, 16-18, 20].

In this study, the effects of normal load and sliding speed have been investigated for a series of Ti pins coated with TiC, when sliding against hardened steel disks in room temperature ambient conditions. The TiC composite coatings were carried out by the Tungsten Inert Gas (TIG) welding torch melting method. On the basis of experimental results, wear mode and wear mechanism maps have been constructed. The observed wear modes and wear mechanisms are discussed with respect to the tribo-oxidation effects, role of material transfer, and effect of third body in the contact.

2. Experimental

Dry unidirectional sliding wear tests were carried out under the ambient conditions at room temperature on a Pin-On-Disk (ASTM 99-05) apparatus Fig. 1. Cylindrical Ti pins of 4.3mm diameter, coated with TiC composite coatings pins, with flat ends, apparent area of contact ($1.44m^2$ x 10^{-5}), were used as tests specimens. Hardened steel disks of 75mm outer diameter 3.8mm thickness used as the counter-face for testing coated pins. The normally

loaded stationary pins were slid against rotating disk in dry sliding conditions at room temperature. The sliding distance was kept constant for all tests. The tests were carried out at different constant sliding speeds, 0.38, 0.5, 0.86, 1.2 and 1.5m s^{-1} by varying normal loads in increments of 10 N, from 10 to 50N for apparent contact pressure range of 694 to 3,472kPa respectively. The sliding distance was 5,560m and the numbers of revolutions were 30,000 for each combination of sliding speed and normal load. A new disk and pin pair was used for each test.

A 20kg load cell was used to measure the frictional force between pin and disk mating surfaces during the sliding. An analytical balance with accuracy of 0.01 mg was used to evaluate mass loss following exposure. The wear rates (m^3m^{-1}) were calculated by converting mass loss to volume loss from the densities of both materials and then dividing the volume loss by the total sliding distance. SEM microscopy and EDX analysis of the worn surfaces and wear debris were carried out following each test to study the wear modes and wear mechanisms of these materials against each other. The densities of Ti base TiC composite coatings and hardened gauge plate were 4.92g cm^{-3} and 7.8g cm^{-3} respectively. The wear rates (m^3 m^{-1}) of the both materials were calculated on the basis of these densities. Repeat tests were carried out to check the reproducibility of the experiments. Experimental error was calculated for the Ti base TiC composite coatings for three tests (n=3) at sliding speed 0.5 $m.s^{-1}$ and normal load 50N which was found % Fig. 3. The average surface roughness of the hardened gauge plate disks and Ti base TiC coatings pins were Ra 0.559µm and Ra 0.367µm respectively.

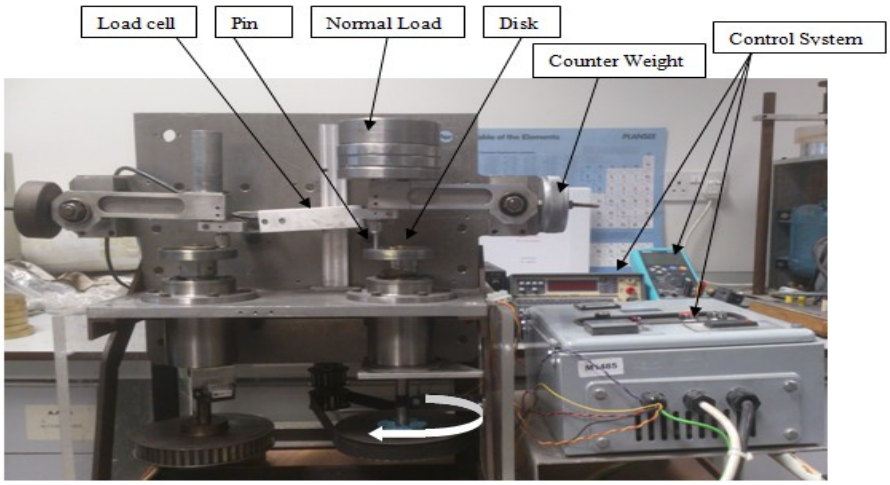

Fig. 1 Pin-on-disk tribometer (dry sliding wear testing rig).

2.1. Materials

2.1.1. Table 1 shows the chemical composition of the steel (A.I.S.I. 0-1- Ground Flat Stock), provided by the steel supplier, which is used as disks material. The hardness value of the hardened steel disks is 700 HV5.

Table 1 The chemical composition of the steel (A.I.S.I. 0-1-Ground Flat Stock) disk

Element	**Weight %**	**Element**	**Weight %**
C	0.95	**V**	0.20
W	0.50	**Si**	0.25
Cr	0.50	**S&P up to**	0.035
Mn	1.20	**Fe**	96.37

2.1.2. Pin material

Titanium base TiC composite coating was used as pin samples. The hardness value of titanium base titanium carbide coatings was 383 HV5.

2.2. TIG coating procedure

The TIG welding torch melting process was used to produce Ti base TiC composite coatings. The steps in preparing specimens for testing are described as follows:

2.2.1. Ti surface preparation

Titanium samples were ground with Grit 120 emery paper by using grinding machine to make rough surface. These samples were washed / cleaned by using soap and acetone to remove any contamination and dried using an air dryer.

2.2.2. TiC powder deposition

Titanium Carbide, TiC – 140, + 325 mesh, typically 99.5% pure powder, 1mg mm^{-2}, was placed on a clean Ti substrate. 5 drops of PVA (polyvinyl acetate) binder along with Alcohol were added to the powder and mixed by water. The paste was spread equally on the substrate surface and flattened using a hard plastic sheet. These samples were dried subsequently in order to evaporate the alcohol, and were placed in an oven at $80^{o}C$ for 1 hour to remove all moisture from the powder mixture on the surface of the substrate.

2.2.3. Tungsten Inert Gas (TIG) welding torch melting process of coating of TiC coatings on Ti substrate

For coatings on the titanium substrate, a TIG 165 DC/HF welding machine was used. TiC ceramic powder of 99.5% purity having nominal size between 45 and 100 micron supplied by Meterion Inc., USA, was used as the reinforcing powder for coating. Metal matrix composite melt tracks were produced using TIG 165 machine with a 2.4 mm in diameter of non-consumable thoriated tungsten electrode. A working distance of 1mm was measured at the end of electrode tip to the surface of dried coating before the melting commenced. The

heat input for melting the track under the torch was generated at 30 V at 90A current with the (table travelling speed) melting speed 1 mm s^{-1} to produce 50% overlapped TiC coatings tracks. These overlapped/multi-pass tracks were produced in one single direction. The direction and distance of travelling were controlled using simple numerical control. TIG welding torch melting efficiency of heat absorption was considered to be 48% [21]. The samples were shielded using argon gas at 20 lit./min. which was streamed while producing the track layers to prevent excessive oxidation. After coating, those samples were ground on grinder machine and then cut into pin size 4.3 mm diameter on EDM wire cut machine. The micrograph and EDX analysis of the coated sample is shown Fig. 2. The average thickness of the finish surface of the coatings was 0.633mm Fig. 12(a).

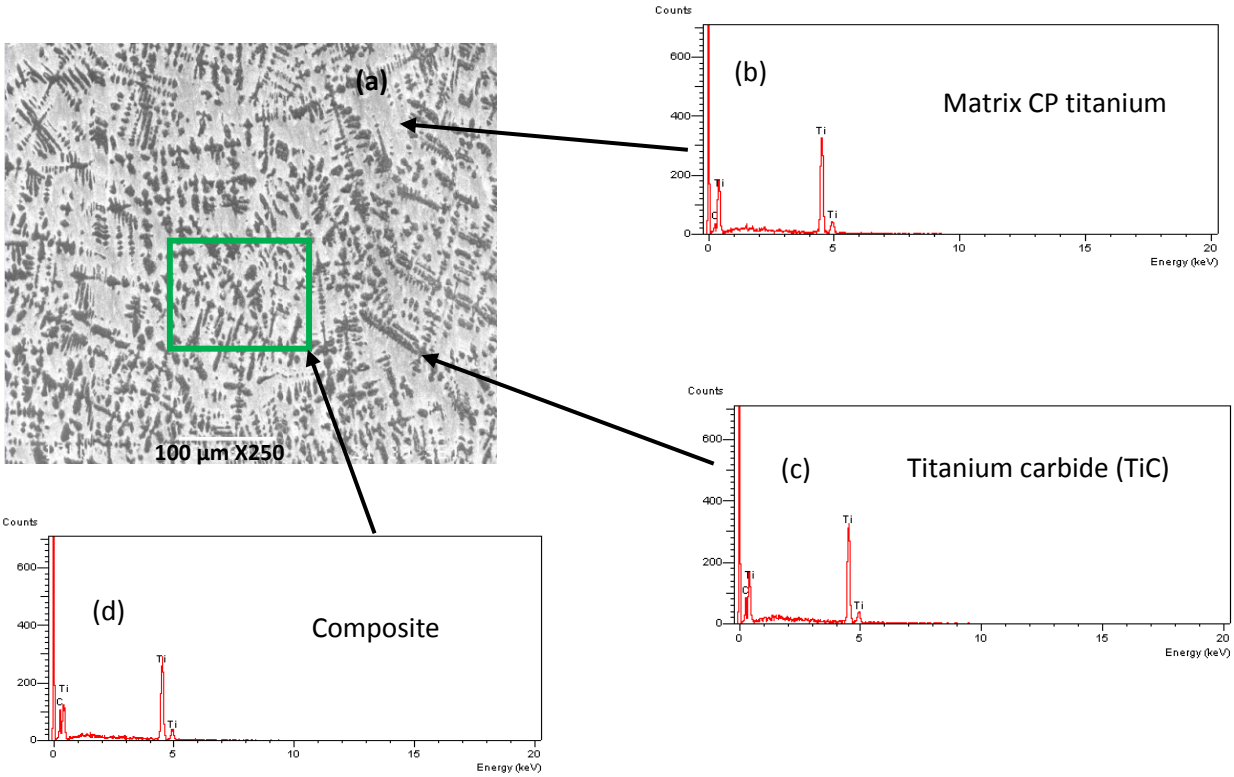

Fig. 2 (a) The micrograph of the CP titanium base TiC coating surface, b) the EDX analysis of the CP titanium matrix (substrate), c) the EDX analysis of the Titanium carbide (TiC) and d) the EDX analysis of the titanium carbide composite coatings.

2.3. Experimental error

The experimental error, Fig. 3, for Ti base TiC composite coatings pins against hardened steel disks, calculated on the basis of repeat tests carried out at sliding speed 0.5m s^{-1} and normal load 50N (number of tests, n =3). The experimental error ±8% was found for the Ti base TiC coatings pins against hardened steel disks.

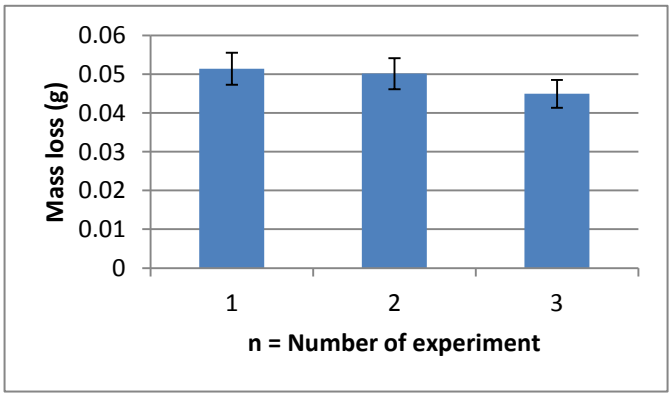

Fig. 3 Experimental error (±8%) for the TiC coatings pins against hardened steel disks.

3. Wear tests results

3.1. Wear rate of TiC/Ti coating pin against hardened steel disks

Fig. 4 shows the wear rate comparison of TiC composite coatings pins and hardened steel disks at various constant sliding speeds for the range of normal loads. The trends from the results indicate that the ranking order of wear resistance of the two materials changed as a function of load and speed. At the two extremes of conditions, Fig. 4(a), higher loads and speeds, and Fig. 4(d), lower loads and speeds, the TiC coatings provided greater wear resistance than the counterface. However, the situation reversed at highest loads, Fig. 4(e).

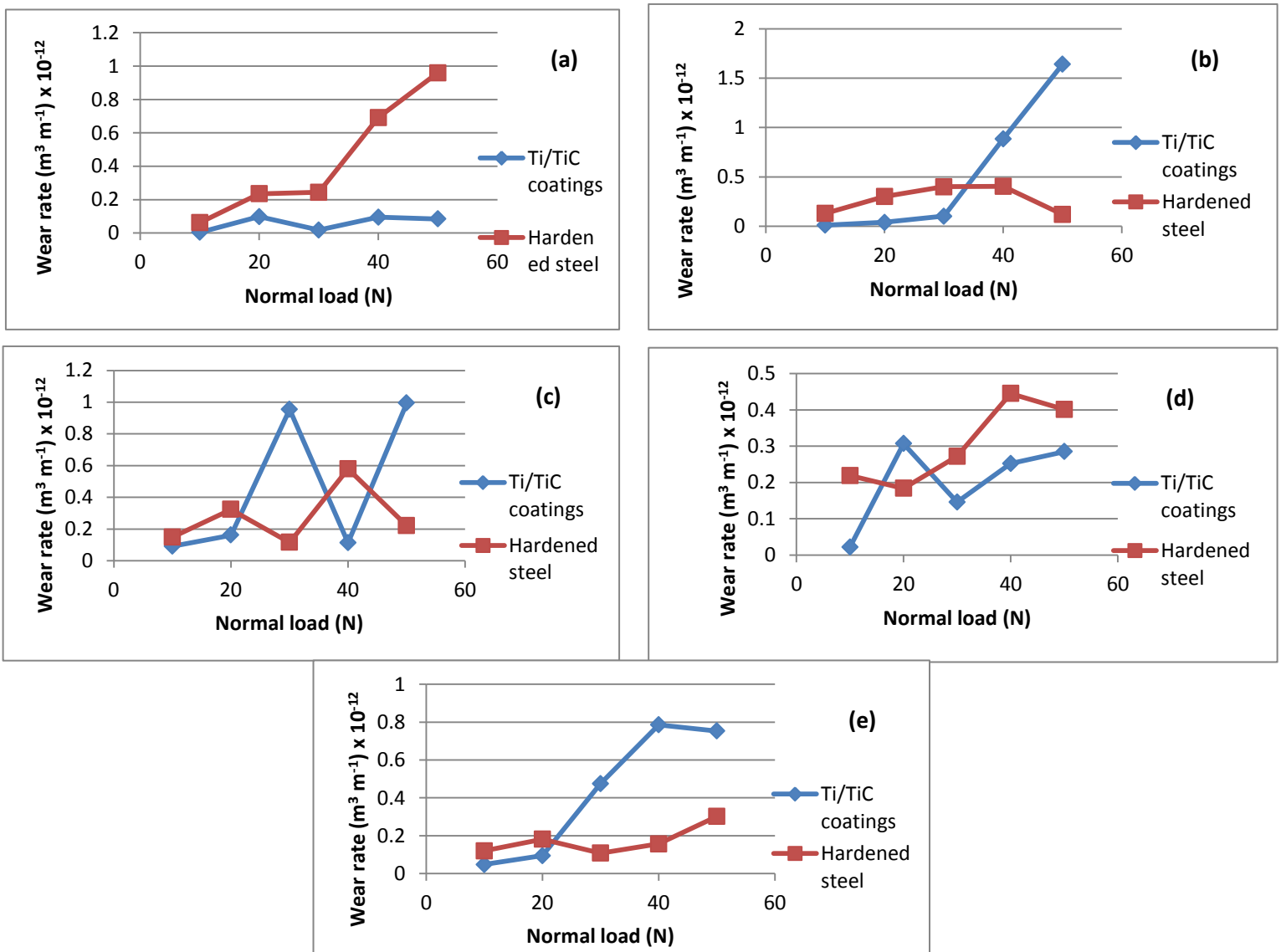

Fig. 4 Wear rate comparison of TiC coatings and hardened steel, (a) at sliding speed 0.38ms^{-1} and various normal load, (b) at sliding speed 0.5ms^{-1} and various normal load, (c) at sliding speed 0.86ms^{-1} and various normal load, (d) at sliding speed 1.2ms^{-1} and various normal load, and (e) at sliding speed 1.5ms^{-1} and various normal load.

Fig. 5 shows the wear rate of TiC composite coatings pins against hardened steel disks at constant sliding speeds and normal loads. As it is seen from Fig. 5(a), at sliding speed 0.5m s^{-1}; wear mode regime transitions occurred from very mild wear to mild wear then further to medium wear with the increase of normal load possibly due to greater removal rate of the oxide than that of the rate of oxidation. For the effect of sliding speed, transitions were observed at intermediate speeds, with the transition speed decreasing with increases in load, Fig. 5(b).

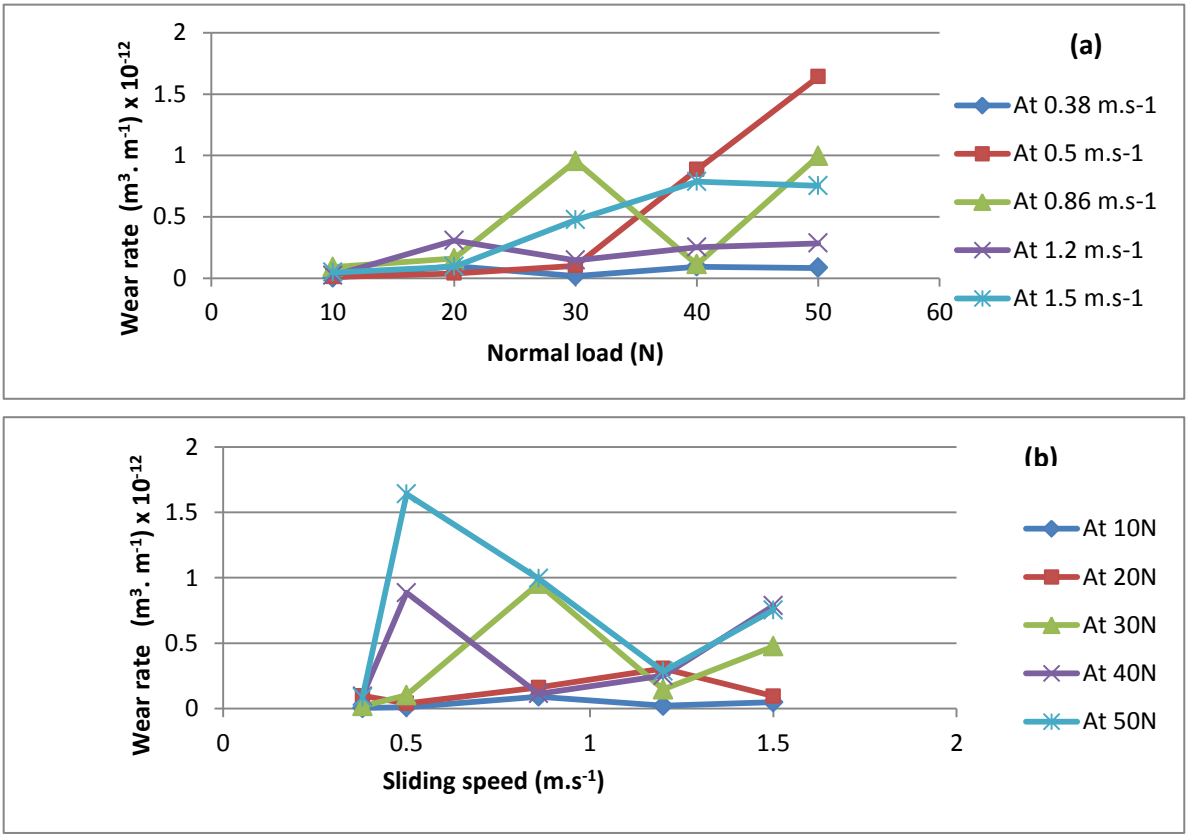

Fig. 5 (a) Wear rate vs normal load of TiC coated pins against hardened steel disks and (b) wear rate vs sliding speed of TiC coated pins against hardened steel disks.

Fig. 6 shows the wear rate of hardened steel disks against TiC composite coatings pins at constant sliding speeds and normal loads. Transitions in wear regimes were observed at intermediate loads and speeds, consistent with tribo-chemical effects on the surface.

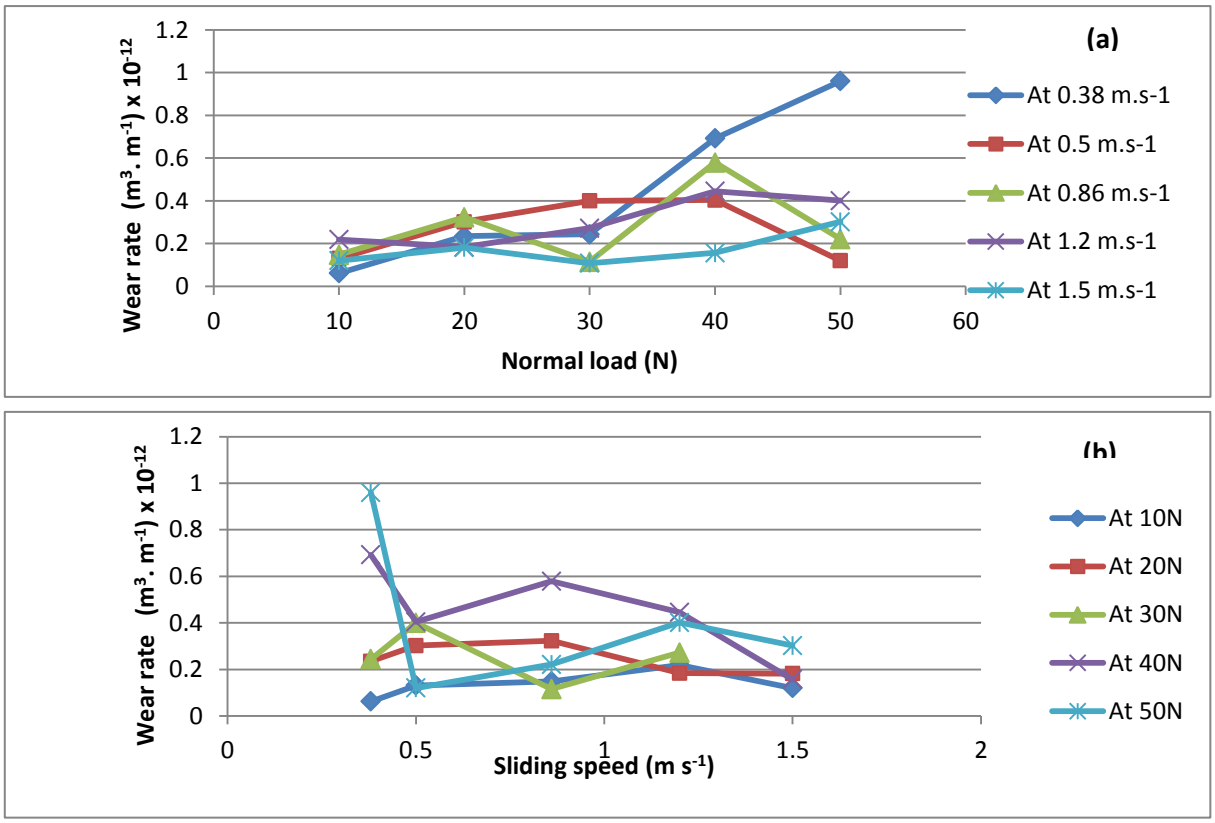

Fig. 6 (a) Wear rate vs normal load of hardened gauge plate disks against TiC coated pins and (b) wear rate vs sliding speed of hardened gauge plate disks against TiC coated pins.

Fig. 7 shows the total mass loss of the TiC composite coated pins and hardened steel disks at constant sliding speed for the range of normal loads for the total sliding distance 27,800m for each sliding speed.

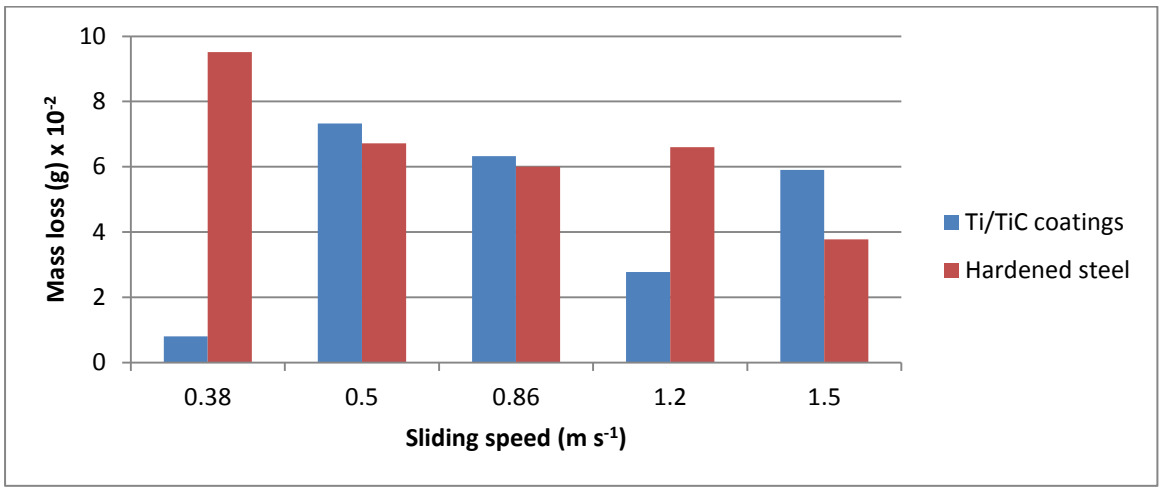

Fig. 7 The total mass loss comparison of hardened steel disks and Ti base TiC coatings pins

SEM micrographs and EDX analysis, Figs. 8 & 9 indicate that significant oxidation of the disks occurred and that iron oxide was transferred to the pin mating surface in the sliding contact.

There was a general trend for greater oxidative wear debris formation as a function of increases of sliding velocity for both pin and disk. As the sliding speeds increased for both pin and disk, Figs 8(a-b), the presence of oxide increased. This layer appeared to reduce in more severe conditions i.e. at higher sliding speeds and loads for the pin material, Figs 8(c-d). By contrast, for the disk materials, abrasive wear was more in evidence in these conditions, with significant ploughing of the surface observed.

Clearly, the wear mechanisms for both pin and disk vary significantly, depending on the applied load and sliding velocity for both coated and uncoated materials. This is addressed further in the Discussion below.

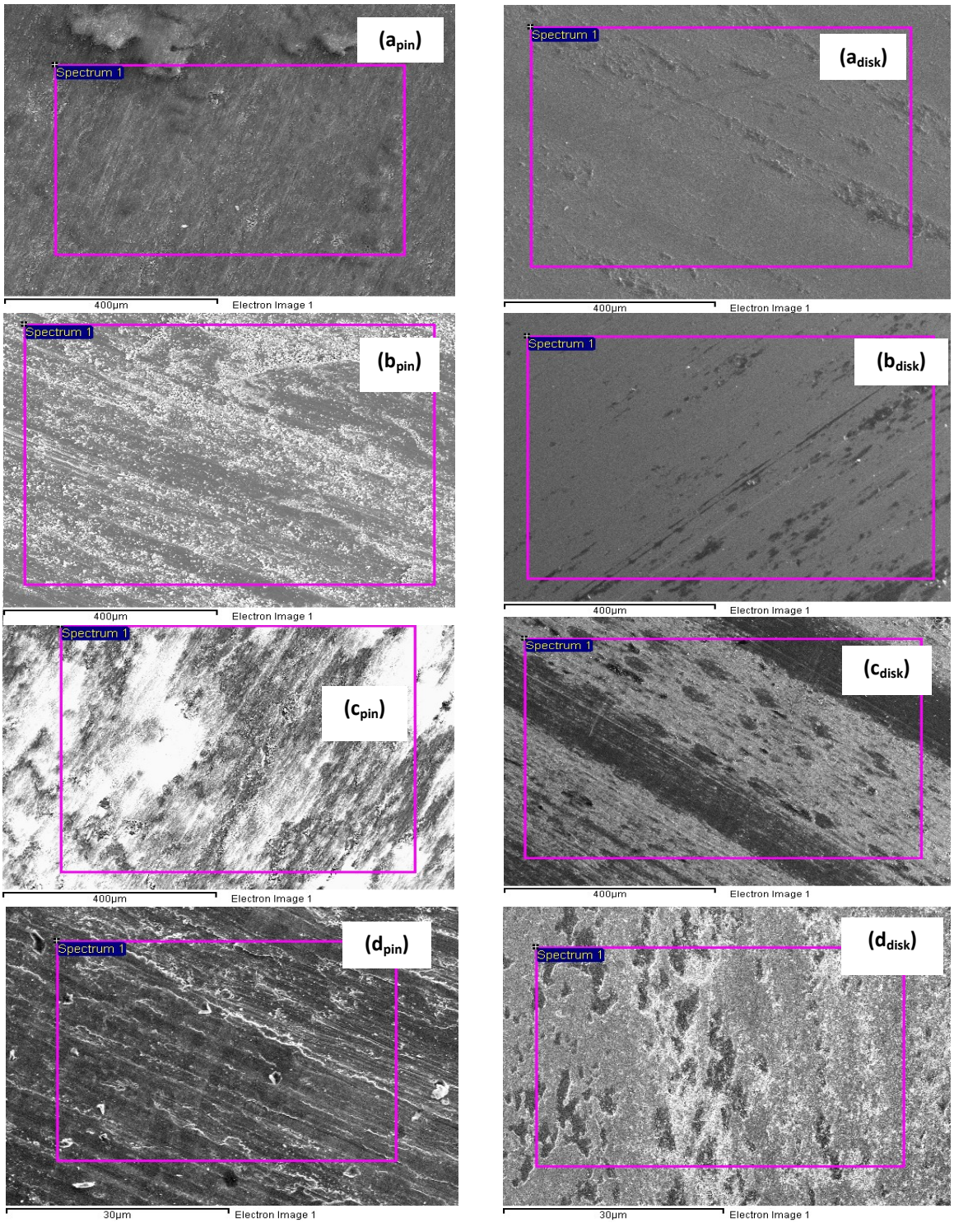

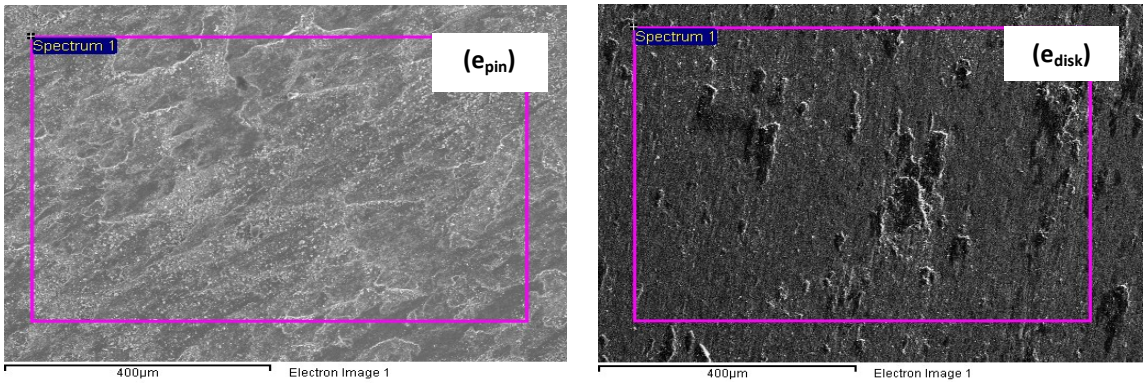

Fig. 8 SEM micrographs of the worn surfaces of the TiC coatied pins and wear track of the hardened steel disks, (a) at) at normal load 30N and sliding speed 0.38m s^{-1}, (b) at 50N and 0.5m s^{-1}, (c) at 40N and 0.86m s^{-1}, (d) at 50N and 0.86m s^{-1} and (e) at 50N and 1.5m s^{-1}.

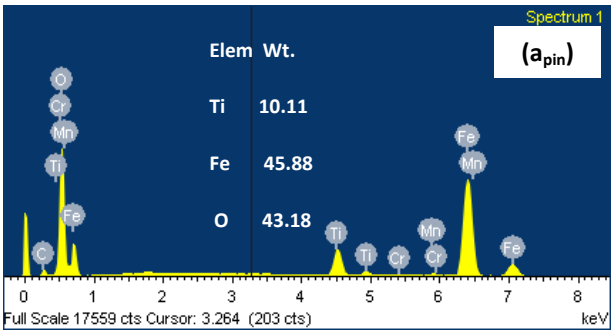

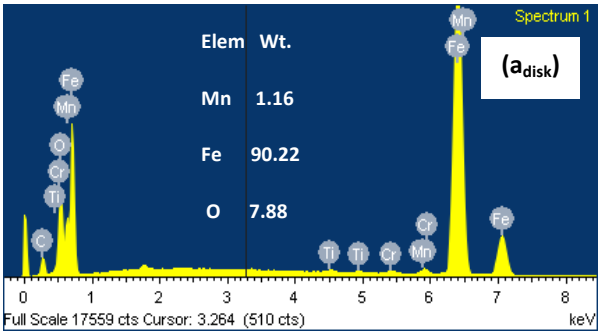

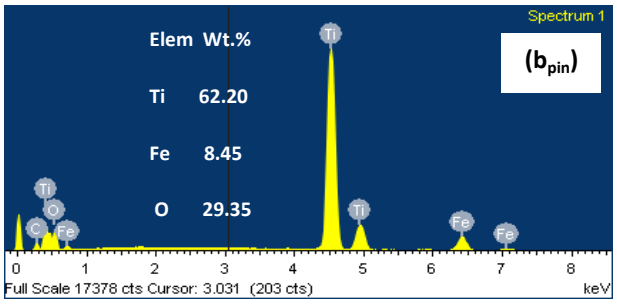

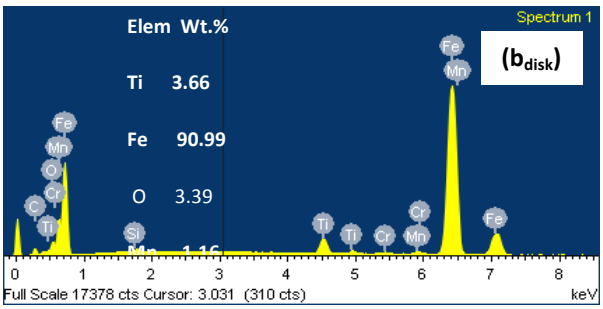

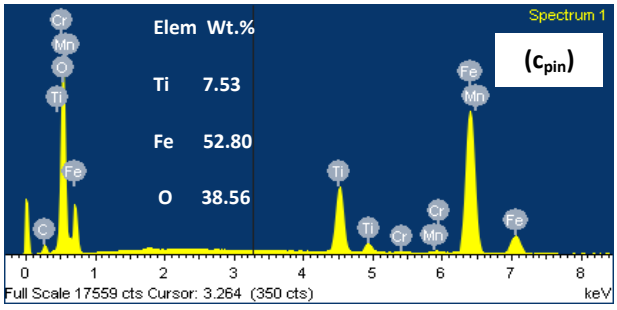

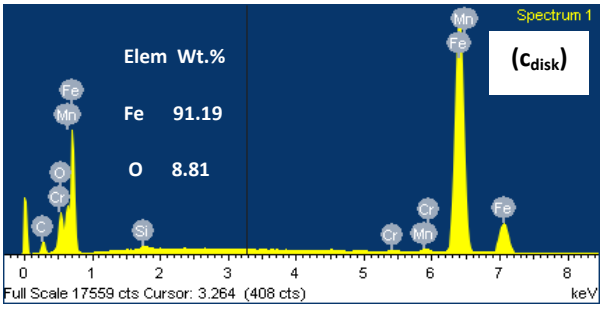

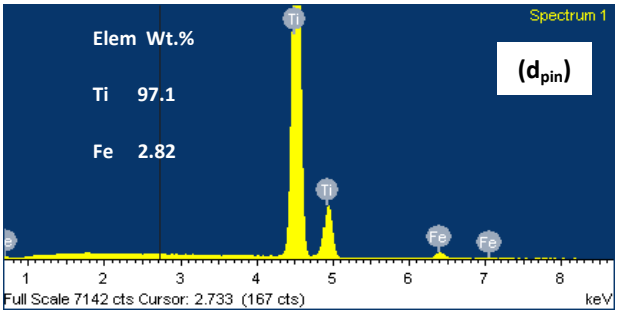

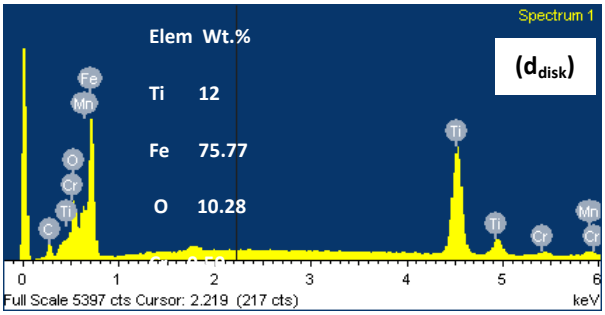

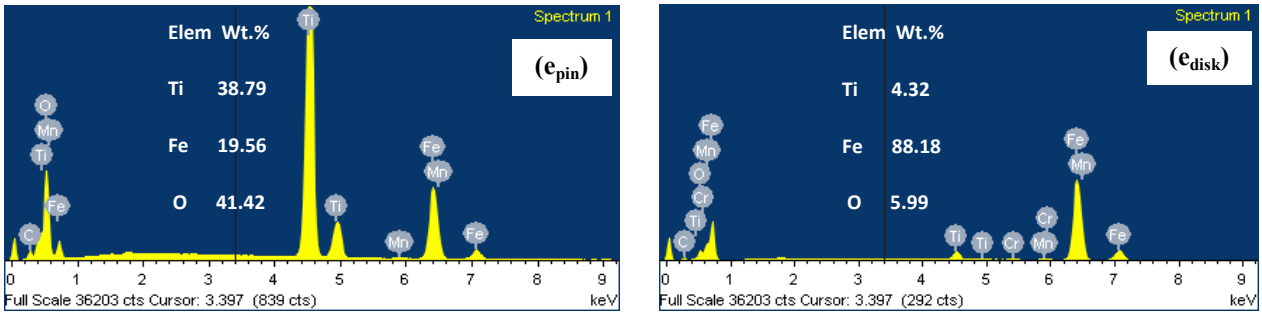

Fig. 9 EDX analysis of the worn surfaces of the TiC coatings pins and wear track of the hardened steel disks, (a) at) at normal load 30N and sliding speed 0.38m s^{-1}, (b) at 50N and 0.5m s^{-1}, (c) at 40N and 0.86m s^{-1}, (d) at 50N and 0.86m s^{-1} and (e) at 50N and 1.5m s^{-1}.

Figs. 10 & 11 Show the SEM micrographs and EDX analysis of the wear debris respectively. The shape of the wear debris changed with the increase in sliding speed. Compacted powder wear debris arose from the counterface at lower normal loads Figs. 10(a-b, d, g) and from Ti base TiC composite coatings pins at higher normal loads 10(e-f, h) for the range of sliding speeds. The flakes like wear debris were generated from hardened steel disks Figs. 10(c, g). From EDX analysis Fig. 11(a-h), the wear products mainly consisted of Ti, O and Fe in all cases. Thus, oxides of both titanium and iron were present in the wear debris.

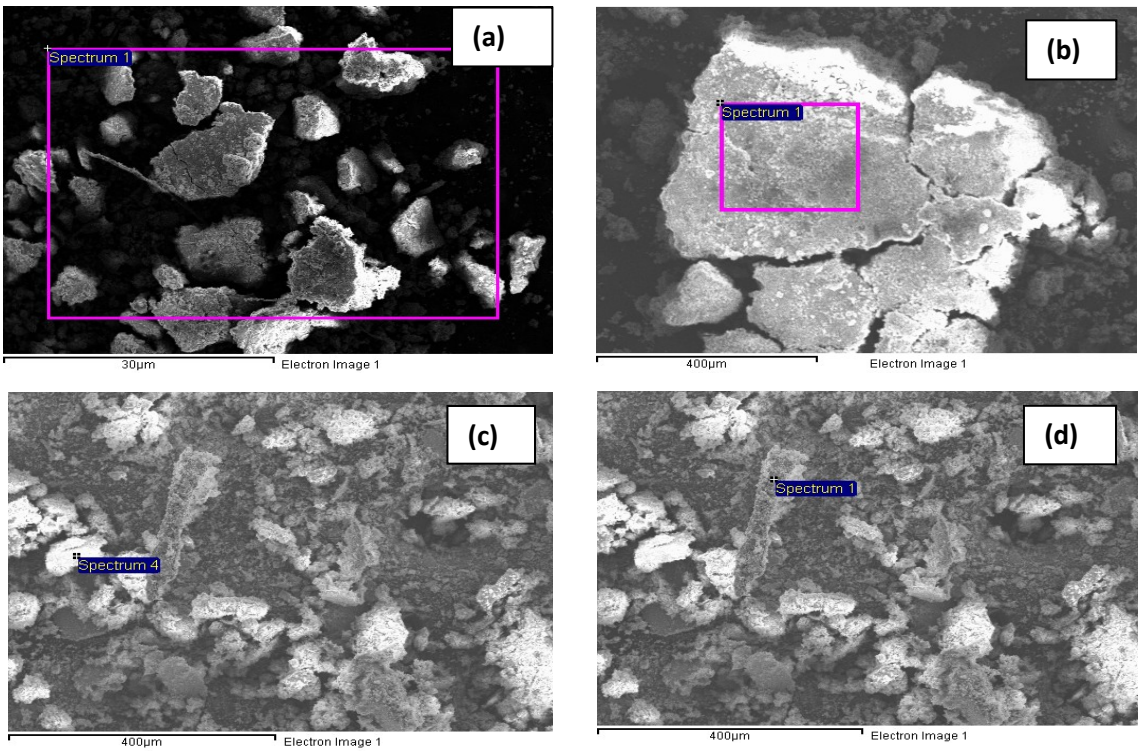

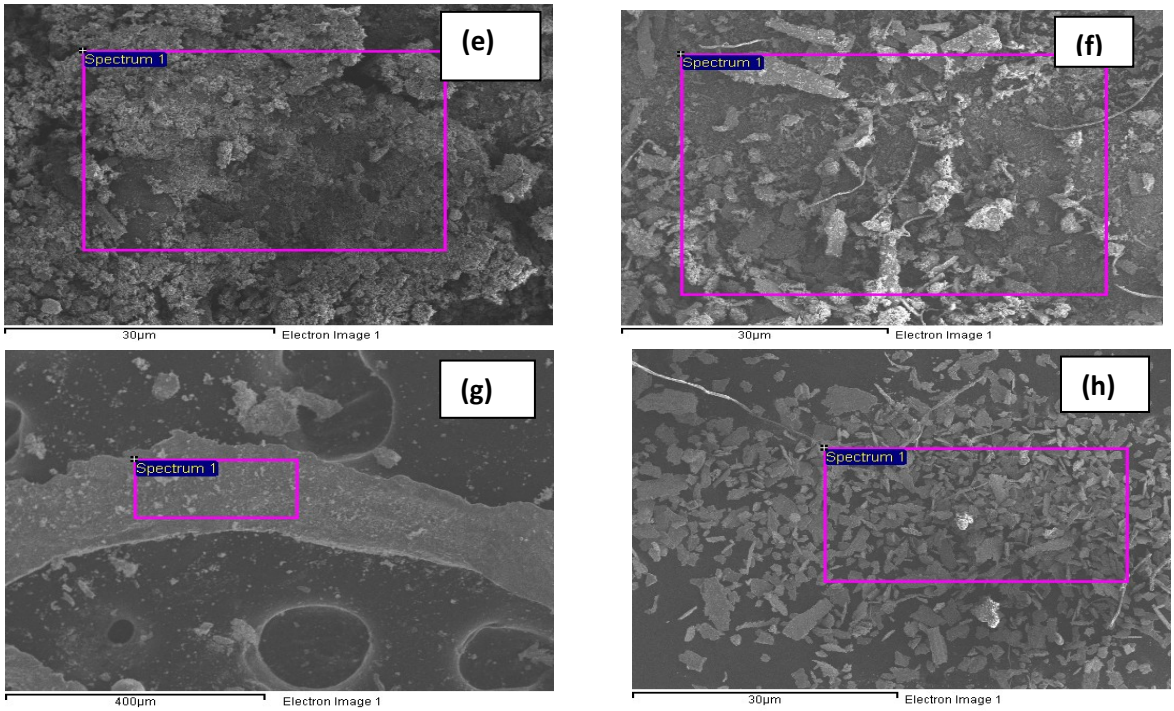

Fig. 10 SEM micrograph of wear debris of TiC coatings against hardened gauge plate (a) at sliding speed 0.38m s^{-1} and normal load 30N, (b) at 0.38m s^{-1} and 30N at high magnification, (c) at 0.5m s^{-1} and 40N point analysis, (d) at 0.5m s^{-1} and 40N point analysis, (e) at 0.5m s^{-1} and 50N, (f) at 0.86m s^{-1} and 50N, (g) at 1.2m s^{-1} and 20N high magnification, and (h) at 1.5m s^{-1} and 50N.

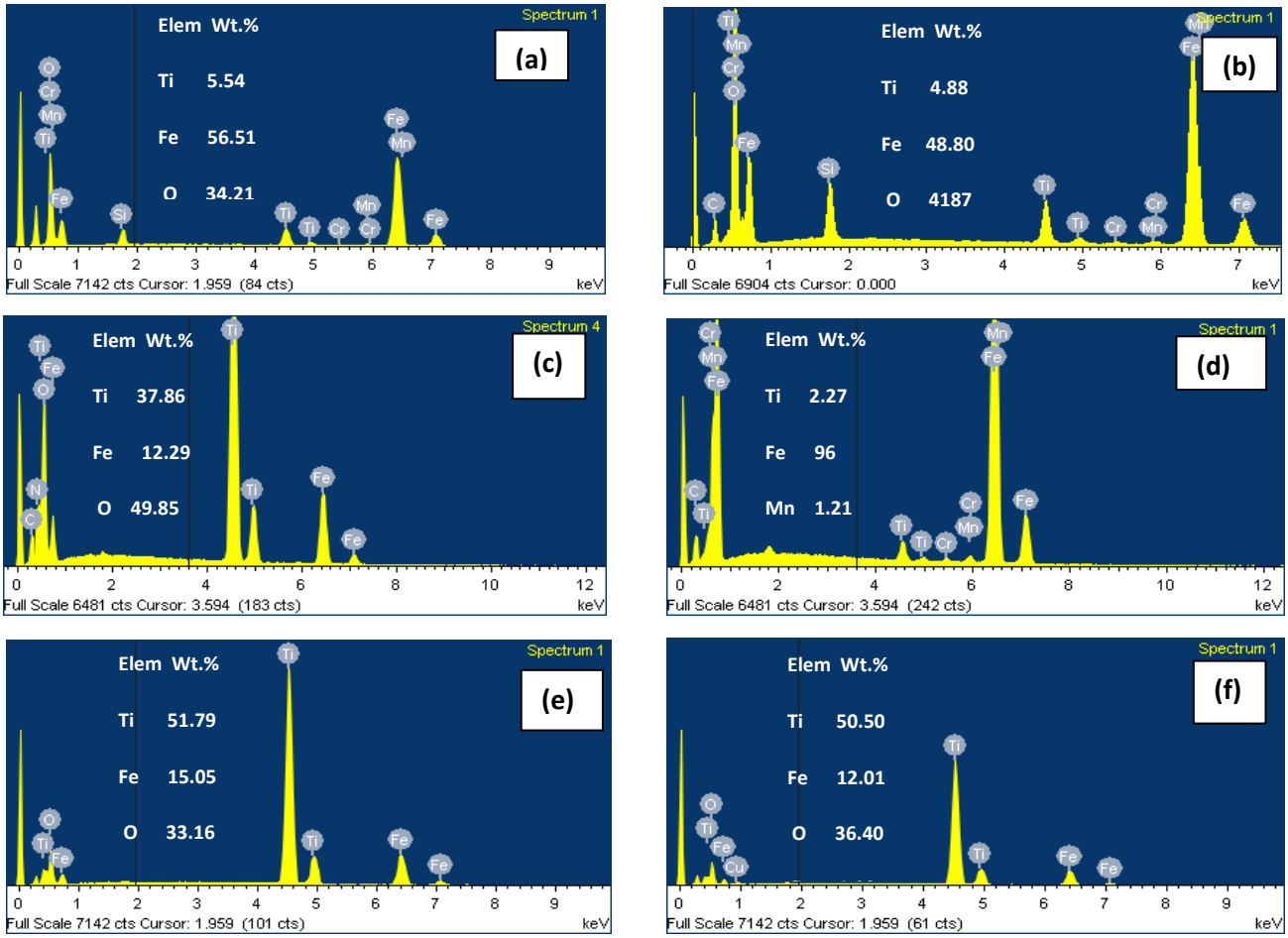

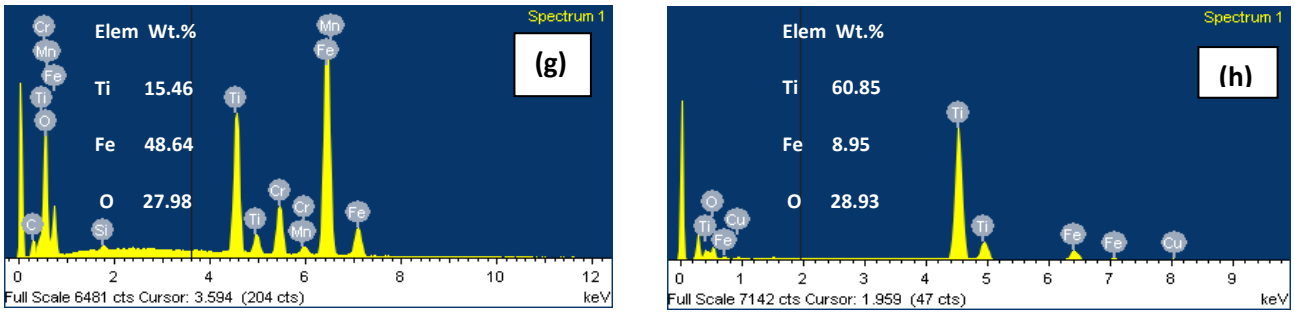

Fig. 11 EDX analysis of wear debris of CP-Ti base TiC coatings against hardened gauge plate (a) at sliding speed 0.38ms^{-1} and normal load 30N, (b) at 0.38m s^{-1} and 30N at high magnification, (c) at 0.5m s^{-1} and 40N point analysis, (d) at 0.5m s^{-1} and 40N point analysis, (e) at 0.5m s^{-1} and 50N, (f) at 0.86m s^{-1} and 50N, (g) at 1.2m s^{-1} and 20N high magnification, and (h) at 1.5m s^{-1} and 50N.

Fig. 12(a) shows the thickness of TiC coating before dry sliding test carried out and Fig. 12(b-c) show the thickness of coating left on the worn surface.

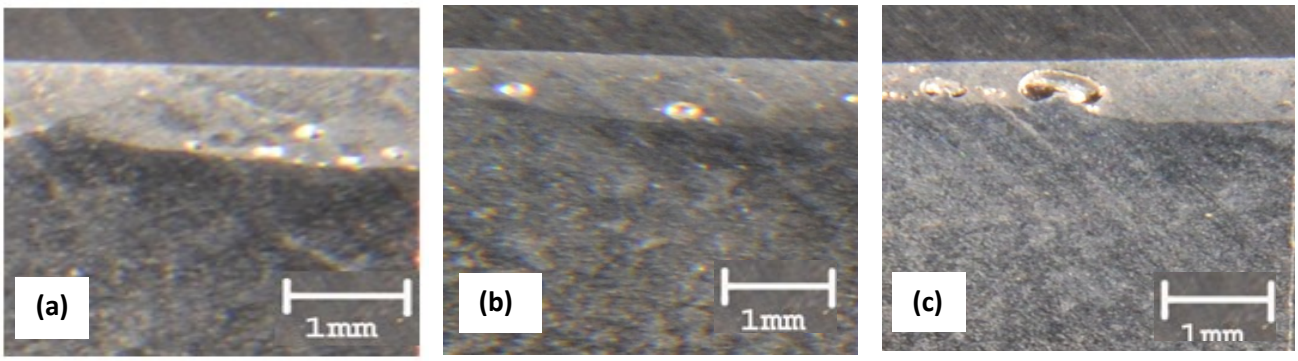

Fig. 12 Cross sectional optical micrographs of Ti base TiC coatings pins, a) thickness of the coatings layer after grinding the coatings surface, b) thickness of the coatings layer after test at sliding speed 1.2m s^{-1} and normal load 50N and c) thickness of the coatings layer after test at sliding speed 1.5m s^{-1} and normal load 40N.

4. Discussion

The higher wear resistance of TiC composite coatings against hardened steel, Fig. 4(a-e), at lower sliding speeds and applied loads is attributed to the load bearing capacity of the TiC composite coatings. In such conditions, an iron oxide layer forms on the contact surface of the coatings. This results in very mild wear rate of the coating. The transfer of iron to the pin material results in the higher wear rate of the counterface and oxidation of the counterface predominates for these combinations of sliding speed and normal loads.

The wear mechanisms of this tribo-couple are modified as the sliding conditions are varied Figs. 5 and 6. The transitions in dominant wear mechanism and in the associated wear rate vary as a function of normal load and sliding velocity, Figs. 8-11. The main factors that control the basic wear mechanisms are contact stresses, temperature and oxidation phenomena. These three factors are interrelated and influenced by both normal load and sliding speed, which make sliding wear complicated [36]. It is interesting that the peak in the

wear rate as a function of sliding velocity changes with increases in load and material composition, Fig. 4. In the former case, such transitions have been associated with the formation of a tribo-oxidative “protective film” on the surface; in the latter case, the shift in peak to higher temperature for the titanium oxide by comparison to that for oxides of iron may be due to a combination of differing mechanical properties of the oxides, i.e. hardness and toughness, and different adhesion and cohesion of the film relating to Pilling Bedworth ratios of the metal/metal oxide system. [11, 18, 19].

The fluctuation in the wear rates of TiC coatings and counterface, observed for the range of sliding speeds and normal loads Figs. 5 & 6, is possibly due to the formation of a mechanically mixed layer, oxidation and deformation of the contact surfaces during dry sliding. Increase in sliding speeds or/and normal load results in increase in flash temperature, frictional heating, oxidation and decrease in yield strength of the mating surfaces. The increase in oxidation with temperature possibly results in the significant decrease in the rate of wear, Fig. 8(c_{pin}) and 9(c_{pin}), and consistent with reports from the other studies [18]. The increase in normal load leads to adhesive wear by material transfer and plastic deformation which results in a significant increase in the rate of wear Fig. 8(b_{pin}, c_{pin}, d & e). A similar trend of wear is observed for wear of TiC coatings in previous work [19] and in the literature for composite coatings irrespective of coating deposition method [10, 25--29, 34].

4.1. Wear maps

Wear maps can represent the mechanistic changes on the worn surfaces of material and the counterpart over a range of operating conditions [22]. Knowledge of both wear mode and wear mechanisms of the material of the worn surface and counterface is also essential in order to understand the material degradation mechanisms and chemical effects in the contact [17]. Wear mode maps identify the mode of degradation and establish the level of wastage rate and potential ‘‘safe’’ and “unsafe” operation conditions for materials [23]. Wear mechanistic maps show the different wear mechanisms for different materials in tribological contact, on the basis of experimental observations [13, 24]. Such maps link the observed wear mechanisms to the actual conditions. These maps demonstrate clearly that transitions from one dominant wear mechanism to another may also be identified by changes in measured wear rates [22].

4.1.1. Wear mode regimes and maps

Fig. 13 shows the wear modes maps for both specimens and counterface. The classifications of wear mode into four distinct regimes, namely (a) very mild wear (b) mild wear (c) medium wear and (d) severe wear, has been made on the basis experimental observations and analysis of worn surfaces and wear products. In these conditions, mild wear results in smooth worn surfaces, and dark grey powder like debris – associated with oxidative wear processes. On the other hand, bright, rougher worn surfaces and larger metallic wear debris

are associated with medium wear and severe wear [35]. Wear regimes have been defined studies by the present authors [19, 33]. The wear modes regime limits are as below:

a) Very mild wear ≤ [0.1 (m^3 m^{-1}) x 10^{-12}]

b) [0.1 (m^3 m^{-1}) x 10^{-12}] < mild wear ≤ [1.12 (m^3 m^{-1}) x 10^{-12}]

c) [1.12 (m^3 m^{-1}) x 10^{-12}] < medium wear ≤ [3.35 (m^3 m^{-1}) x 10^{-12}]

d) Severe wear > [3.35 (m^3 m^{-1}) x 10^{-12}]

In these maps, it can be clearly seen that very mild wear is more prevalent with respect to normal load for TiC coated pins Fig. 13(a); for the counterface, mild wear predominates, Fig. 13(b). Medium wear of TiC coatings pin occurs only for one combination of sliding speed and normal load. From Fig. 13(a-b), the combination of the very mild and mild wear zone can be regarded as the safe operation zone for this tribo-couple.

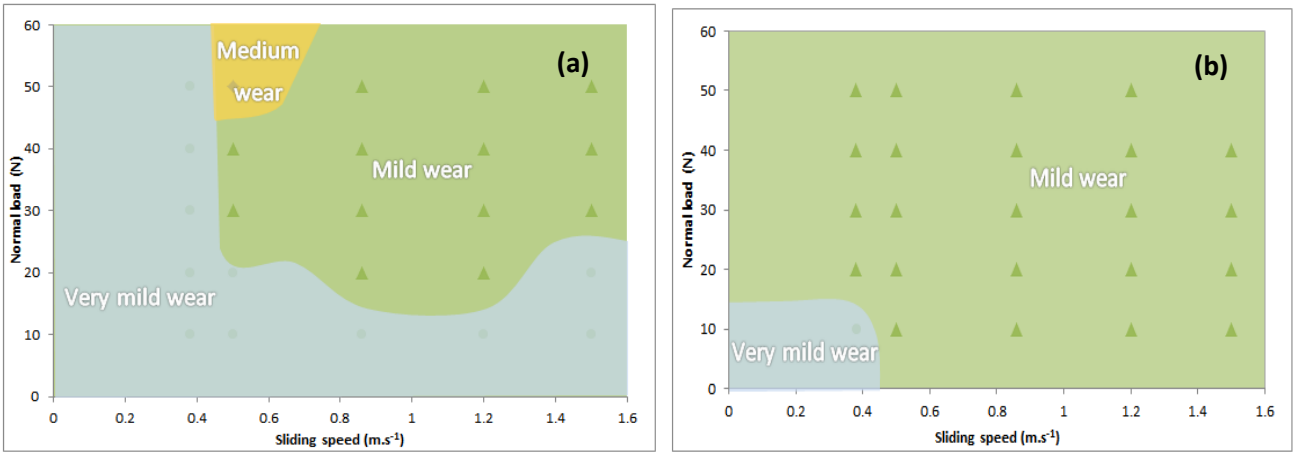

Fig. 13 Wear modes maps, a) TiC/Ti coated pins against hardened steel disks and b) hardened steel disks against TiC/Ti coated pins.

4.1.2. Wear mechanism regimes and maps

Fig. 14 shows the wear mechanism maps of TiC coatings and hardened steel against each other. The wear mechanism regimes can be summarized as:

- Oxidative – adhesive wear
- Adhesive - oxidative wear
- Oxidative – abrasive wear
- Abrasive - oxidative wear
- Micro-abrasion
- Abrasive wear

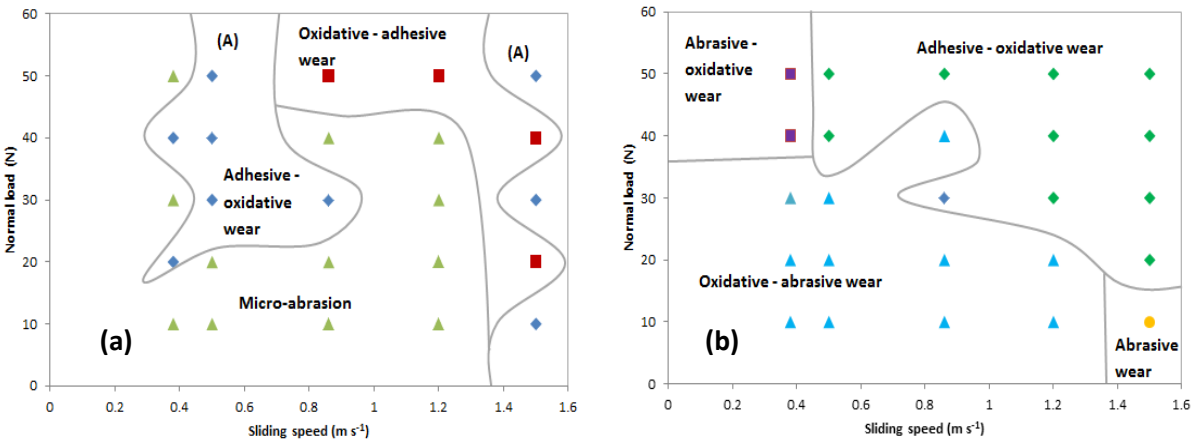

Fig. 14 Wear mechanisms maps, a) TiC/Ti coated pins against hardened gauge plate steel disks, and b) hardened gauge plate steel disks against TiC/Ti coated pins.

From Fig. 14(a), TiC coatings do not appear to have undergone significant tribo-oxidation in the lower sliding speed domain. A so-called "mechanically mixed layer" predominates on the pins surfaces. The wear in this regime is largely controlled by micro-abrasion of TiC by oxide particles in the mechanically mixed layer 8(a & c) and 9(a & c). EDX analysis of the wear debris shows the presence of iron and oxygen, Figs. 11(a, b & g). These observations are in agreement with other findings from the literature HSS [17].

For the ''adhesive - oxidative wear'' regimes, Fig. 14, wear fragments are generated due to adhesion between the sliding contact surfaces, Figs. 8(b_{pin} & e_{pin}) and 9(b_{pin} & e_{pin}). Analysis of wear debris shows the presence of fine compact grey oxide powder and flake like features, Figs. 10(c-e, h) and 11(c-e, h). This suggests tribo-oxidation of the TiC coating [24]. The size of the wear debris is linked to the severity of adhesive wear [30].

In the ''oxidative - adhesive wear'' regime region, Fig. 14(a), due to increase in frictional heat and contact temperature, wear of the TiC coatings occurs through adhesive and delamination mechanisms, Figs. 8(d_{pin}) and 9(d_{pin}), [26] together with oxidative wear mechanism. Increases in frictional heating results in ductility of coatings which result in a transition in wear mechanisms [31]. The presence of larger micro flakes and oxide debris is characteristic of this regime Figs. 10(f) and EDX 11(f). Transitions in wear mechanisms of the metals in sliding contacts have been attributed to their increased sensitivity to the onset of intense shearing, surface sliding temperatures and shear deformation rates, in the wear contact zone [32] in addition to oxidation phenomena and the above maps include such transitions.

4.2. Wear mode maps comparison between TiC/Ti composite coatings against hardened steel counterface and 303SS base TiC composite coatings against alumina counterface

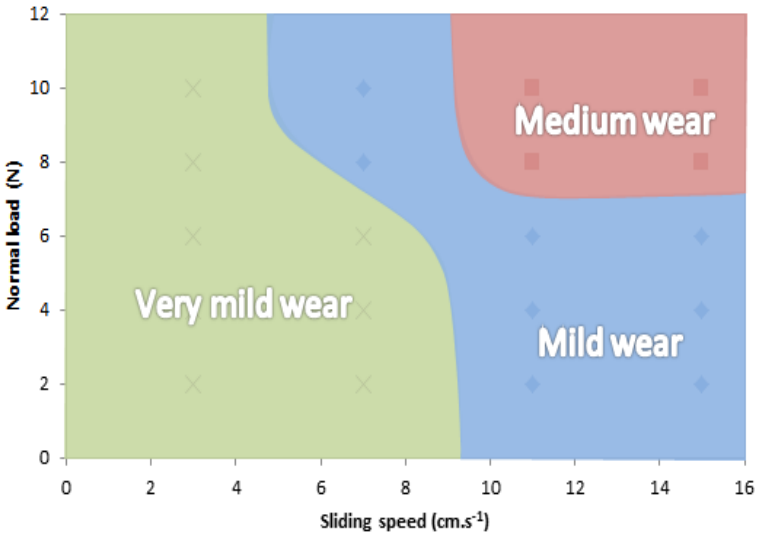

Fig. 15. Wear mode map for TiC composite coatings disk (303 SS base) against alumina ball taken from previous work [19]

Fig. 15 shows the range of sliding speed and normal load of the previous work by the current authors [19] involved in the present study, which can be compared with present work by the current authors. It is clear from this figure that the wear rate of the TiC composite coatings, deposited on 303 SS, is higher than that of the TiC composite coatings using Ti as a base material, Fig. 13(a) for the range of sliding speeds and normal loads of the previous work. The higher wear resistance of the TiC/Ti composite coatings in the present study is attributed to the dense structure with low porosity and absence of cracking Fig. 12, [2] together with more favourable thermal expansion conditions for the Ti/TiC coating system [10].

5. Conclusions

- TiC/Ti composite coatings were produced by a TIG welding torch melting method and tested for dry sliding wear against hardened steel to investigate the change in wear modes and wear mechanisms at various sliding speeds and normal loads under dry sliding conditions.
- The sliding wear of TiC hard coatings can change significantly with variation of parameters such as normal load and sliding speed.
- Significant levels of iron oxide were transferred to TiC coatings pins at lower sliding speed while some transfer of pin material to disks occurred at higher sliding speeds and normal loads due to increases in frictional heat.
-

Acknowledgements

We would like to thank International Islamic University Malaysia (IIUM) for providing the test specimens to perform the present work and to the Leverhulme Trust for sponsorship of the work –grant RL7583- 2012-2013.

References

[1] S. Krol, L. Ptacek, M. Hepner, Friction and wear properties of titanium and oxidised titanium in dry sliding against hardened C45 steel, Journal of Materials Processing Technology, 157-158 (2004) 364-369.

[2] A. Monfared, A. H. Kokabi, S. Asgari, Microstructural studies and wear assessments of Ti/TiC surface composite coatings on commercial pure Ti produced by titanium cored wires and TIG process, Materials Chemistry and Physics,137 (2013) 959-966.

[3] C. Richard, C. Kowandy, J. Landoulsi, M. Geetha, H. Ramasawmy, Corrosion and wear behaviour of thermally sprayed nano ceramic coatings on commercially pure Titanium and Ti-13Nb-13Zr substrate, International journal of refractory metals & hard materials,28 (2010) 115-123.

[4] J. Oh, S. Lee, Correlation of microstructure with hardness and fracture properties of (TiC,SiC)/Ti-6Al-4V surface composites fabricated by high-energy electron-beam irradiation, Surf. Coat. Technol., 179 (2004) 340-348.

[5] F. Wang, J. Mei. X. Wu, Direct laser fabrication of Ti6Al4V/TiB, J. Mater.Proc. Tech., 195 (2008) 321-326.

[6] E. Bemporad, M. Sebastiani, F. Casadei, F. Carassiti, Surf., Modelling production and characterisation of duplex coatings (HVOF and (PVD) on Ti–6Al–4V substrate for specific mechanical applications, Surf. Coat. Technol., 201 (2007) 7652-7662.

[7] S. Mridha, H . S. Ong, L. S. Poh, P. Cheang, Intermetallic coatings produced by TIG surface melting, J. Mater. Proc. Technol. 113 (2001) 516-520.

[8] S. Mridha, Titanium nitride layer formation by TIG surface melting in a reactive environment, J. Mater. Proc. Technol. 168 (2005) 471-477.

[9] Ali Shanaghi, Paul K. Chu, Ali Reza Sabour Rouhaghdam, Ruizhen Xu, Tao Hu, Structure

and corrosion resistance of Ti/TiC coatings fabricated by plasma immersion ion implantation and depsitin on nickel-titanium, Surface and coatings Technology, 229 (2013) 151-155.

[10] S. Bahadur, Chien-Nan Yang, Friction and wear behaviour of tungsten and titanium carbide coationgs, Wear, 196 (1996) 156-163.

[11] N. C. Welsh, Tribo-metallographic behaviour of high carbon steel, Philos. Trans. R. Soc., Ser. A 257 (1965) 31-50.

[12] S. C. Lim, M.F. Ashby, Overview no. 55 wear-mechanism maps Acta Metall. 35 (1987) 1-24.

[13] H. Kato, T. S. Eyre and B. Ralph, Wear mechanism map of nitride steel, Acta Metall. Mater. 4 (1994) 1703-1713.

[14] P. Gautier and K. Kato, Wear mechanism of silicon nitride, partially stabilized zirconia and alumina in unlubricated sliding against steel, Wear, 162-164 (1993) 305-313.

[15] J. Zhang and A. T. Alpas, Transition between mild and severe wear in aluminium alloys, Acta Mater., 45 (1997) 513-528.

[16] S. Wilson , A. T. Alpas, Wear mechanism maps for metal matrix composites, Wear 212 (1997) 41-49.

[17] S. Wilson , A. T. Alpas, Wear mechanism maps for TiN-coated high speed steel, Surface and Coatings Technology, 120-121 (1999) 519-527.

[18] M. M. Stack, Mapping tribo-corrosion processes in dry and in aqueous conditions: some new directions for the new millennium, Tribology International, 35 (2002) 681-689.

[19] G. Rasool and M. M. Stack, Wear maps for TiC composite based coatings deposited on 303stainless steel, Tribology International, 74 (2014) 93-102.

[20] T. F. J. Quinn, Physical Analysis for Tribology, Cambridge University Press, Cambridge, 1991.

[21] Mridha, Shahjahan and Idriss, A. N. and Baker, Thomas (2011) ''Incorporation of TiC particulates on AISI 4340 low alloy steel surface via TIG arc melting. In: 14th International Conference on Advances in Materials and Processing Technologies, 2011- 07-13 – 2011-07-16, Istanbul.

[22] C. Y. H. Lim, S. C. Lim, K. S. Lee, Wear of TiC-coated carbide tools in dry turning, Wear, 225-229 (1999) 354-367.

[23] M. M. Stack, W. Huang, G. Wang, C. Hodge, Some views on the construction of bio-tribo-corrosion maps for Titanium alloys in Hank's solution: Particle concentration and applied loads effects, Tribology International, 44 (2011) 1827-1837.

[24] Md. OhidulAlam, A. S. M. A. Haseeb, Response of Ti-6Al-4V and Ti-24Al-11Nb alloys to dry sliding wear against hardened steel, Tribology International, 35 (2002) 357-362.

[25] A. Savan, H. J. Boving, E. Fluehmann and H. E. Hintermann, Increased performance of bearing using TiC-coated balls, Journal DE PhysicsIV, 3 (1993) 943-948.

[26] S. Wilson , A. T. Alpas, TiN coating wear mechanisms in dry sliding contact against high speed steel, Surface Coatings Technology, 108-109 (1998) 369-376.

[27] W. Grzesik , Z. Zalisz, S. Krol, P. Nieslony, Invetgation of friction and wear mechanisms of the PVD-TiAlN coated carbide in dry sliding against steels and cast iron, Wear, 261 (2006) 1191-1200.

[28] L. C. Betancourt-Dougherty, R. W. Smith, Effects of load and sliding speed on the wear behaviour of plasma sprayed TiC-NiCrBSi coatings, Wear 217 (1998) 147-154.

[29] M. Mustafa Yildirim, Soner Buytoz, Mustafa Ulutan, Dry sliding wear behaviour of TIG welding clad WC composite coatings, Applied Surface Science 252 (2005) 1313-1323.

[30] Rabinowicz E., The least wear, wear 100 (1984) 533-541.

[31] N. Chelliah, S. V. Kailas, Synergy between tribo-oxidation and strain rate response on governing the dry sliding wear behaviour of titanium, Wear 266 (2009) 704-712.

[32] S. Wilson, A. T. Alpas, Thermal effects on mild wear transitions in dry sliding of an aluminium alloy, Wear. 225-227 (1999) 440-449.

[33] G. Rasool and M.M. Stack, Mapping the role of Cr content in dry sliding of steels: comparison between maps for material and counterface, Tribology International 80 (2014) 49-57.

[34] L. C. Betancourt-Dougherty, R. W. Smith, Effects of load and sliding speed on the wear behaviour of plasma sprayed TiC-NiCrBSi coatings, Wear 217 (1998) 147-154.

[35] I. A. Inman, S.R. Rose, P.K. Datta, Development of a simple 'temperature versus sliding speed' wear map for the sliding wear behaviour of dissimilar metallic interfaces, wear 260 (2006) 919-932.

[36] I. M. Hutchings, Tribology, Friction and Wear of Engineering Materials, ISBN 034056184X.

[37] K. Kato, in: H. M. Hawthome, T. Trocynski (Eds.) Advanced Ceramics for Structural and Tribological Applications, Proc. 34th Conf. CIM, Vancouver, (1995) 23-36.